Liquid Crystals
Publication details, including instructions for authors and subscription information:
http://www.informaworld.com/smpp/title~content=t713926090

Application of time-resolved fluorescence in the study of lipid aggregates II. Motions and order of pyrene probes in an aligned lyotropic nematic phase

Lennart B.-Å. Johansson[a]; Göran Lindblom[a]
[a] Department of Physical Chemistry, University of Umeå, Umeå, Sweden

To cite this Article Johansson, Lennart B.-Å. and Lindblom, Göran(1986) 'Application of time-resolved fluorescence in the study of lipid aggregates II. Motions and order of pyrene probes in an aligned lyotropic nematic phase', Liquid Crystals, 1: 1, 53 — 62
To link to this Article: DOI: 10.1080/02678298608086489
URL: http://dx.doi.org/10.1080/02678298608086489

LIQUID CRYSTALS, 1986, VOL. 1, NO. 1, 53–62

Application of time-resolved fluorescence in the study of lipid aggregates

II. Motions and order of pyrene probes in an aligned lyotropic nematic phase

by LENNART B.-Å. JOHANSSON and GÖRAN LINDBLOM
Department of Physical Chemistry, University of Umeå, S-901 87 Umeå, Sweden

(*Received 28 August 1985; accepted 16 October 1985*)

Time-resolved polarized fluorescence spectroscopy has for the first time, been applied to the study of chromophores in a macroscopically aligned lyotropic nematic phase. The phase is composed of potassium dodecanoate, potassium chloride and water and contains long rod-like aggregates, that are aligned with their long axes parallel to an applied magnetic field. Pyrene, 1-pyrene dodecanoic acid, 1-dodecylpyrene and 1-palmitoyl-2-(6-pyrenylhexanoyl)-*sn*-glycero-3-phosphoryl-choline are solubilized in these aggregates. The photophysics of these probes is a single exponential and typically between 130 and 200 ns in non-degassed samples. For all the probes the plane of the pyrene molecule tends to be oriented perpendicular to the symmetry axis (C_∞ axis) of the aggregate. The order parameters describing the orientation of the electronic transition dipole moment relative to this axis are typically *c.* −0·05. It is concluded that the translational and the local rotational motions of the probes are fast compared to the fluorescence lifetimes. The correlation times characterizing these motions are shorter than 20 ns. Finally, no slow motions such as fluctuations of the normal to the surface of the rod-like aggregate or a slow wobbling of the C_∞-axis can be detected during *c.* 1 μs.

1. Introduction

Time-resolved fluorescence is applied increasingly to the study of chromophores solubilized in lipid aggregates. In particular lipid membrane systems such as vesicles but also micellar systems have been paid much attention. Direct physico-chemical information of such systems from measurements of fluorescence emission is often not obtained straightforwardly and it is remarkable that a consistent theory dealing with fluorescence on anisotropic systems is of a rather recent date [1–4]. Thus, independently several authors around 1980 derived equations relating the fluorescence anisotropy to the static and dynamic properties of fluorophores in these kinds of systems. In a previous study we also pointed out that information about the geometry of lipid aggregates could be extracted from polarized time-resolved luminescence [5]. Such investigations can be performed provided a probe molecule can be found with the appropriate properties concerning emission lifetime, orientation and dynamics. Here we continue our systematic study of fluorophores solubilized in lyotropic liquid crystals. From a theoretical point of view such investigations are best performed with uniaxial, macroscopically aligned systems. To our knowledge no study of time-resolved fluorescence on an oriented lyotropic liquid crystal has been published before although a paper by Cehelnik *et al.* [6] on a thermotropic liquid crystal was reported

about 10 years ago. In previous publications we have shown that some of the so-called lyotropic nematics, that align in a magnetic field, can be utilized in light spectroscopic studies of various chromophores [7]. The nematic used in this investigation is built up of rod-like aggregates [7] and has the advantage of keeping a constant macroscopical alignment for very long times (*several days*) depending on the composition.

2. Theoretical background

A schematic picture of the macroscopically oriented system studied in this work is shown in figure 1. To obtain information about molecular orientation and motion from a time-resolved fluorescence measurement the emission anisotropy $r(t)$, is usually recorded. This is a convenient parameter, since an explicit expression of $r(t)$ can be derived in terms of motion and orientation for an anisotropic system [1–4]. In this section a brief derivation of $r(t)$ is given, where besides the rotational motion translational motion of the probe is also taken into account. This is necessary for systems composed of curved aggregates and where probe molecules with long lifetimes are used [5]. It is assumed that the uniaxial system is oriented so that its symmetry axis, D, coincides with the Z axis of the laboratory frame, L (cf. experimental section). The excitation light propagates along the X axis and is polarized either along the Z or Y axis. The emitted light is monitored along the Y axis after passing through a polarizer. The transmission axis of the polarizer, **T**, can be rotated in the XZ plane. The intensity of the emitted light, F is conveniently described by [3]

$$F(t) = k\mathbf{T}^{\mathrm{L}}\langle P_{ii}^{\mathrm{L}}\mathbf{Q}^{\mathrm{L}}\rangle\mathbf{T}^{\mathrm{L},t}w(t), \quad i = Z \text{ or } Y. \tag{1}$$

The intensity depends on a two-step process which involves the probability that the chromophore is excited, P_{ii}, and the probability, **Q**, that the fluorophore emits light in a particular direction. In the notation used by us [3, 5] P_{ii} is the ii-element of the absorption transition moment tensor and **Q** is the emission transition moment tensor.

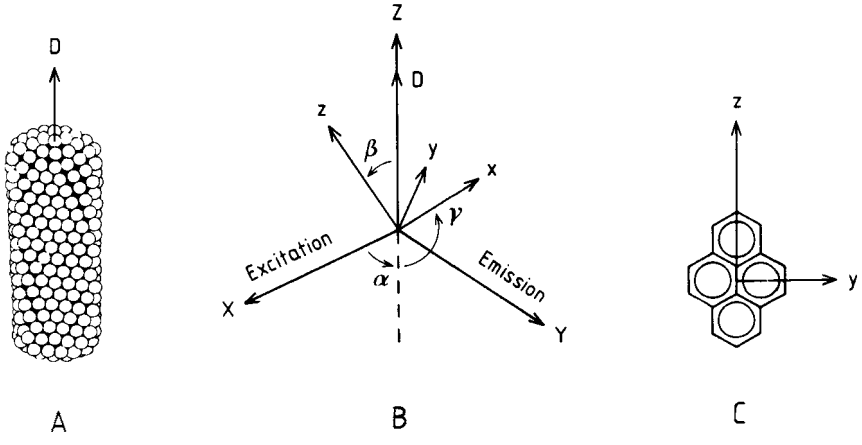

Figure 1. A schematic picture of a polarized emission experiment. (A) Rod-like aggregate of amphiphiles. The uniaxial system investigated here contains such aggregates macroscopically aligned with their long axes (D) mutually parallel. (B) (X, Y, Z) and x, y, z are the laboratory (L) and the molecule (M) fixed coordinate systems. $\Omega \equiv \alpha, \beta, \gamma$, are the eulerian angles of transformation. The excitation beam of light propagates along the X axis and the emission is detected along the Y axis. (C) Pyrene and its molecule fixed frame.

The transmission axis of the emission polarizer is represented by the 1 × 3 matrix **T** and $\mathbf{T}^{\mathrm{t}}$ is the transpose matrix. k is a constant and $w(t)$ is the probability of emission at a time t after excitation. The ensemble average

$$\langle P_{ii}^{\mathrm{L}}\mathbf{Q}^{\mathrm{L}}\rangle = \int_{\Omega_0}\int_{\Omega} f(\Omega_0)\,P_{ii}^{\mathrm{L}}(\Omega_0)\,g(\Omega_0|\Omega, t)\mathbf{Q}^{\mathrm{L}}(\Omega)\,d\Omega_0\,d\Omega, \tag{2}$$

where $f(\Omega_0)$ is the probability density that a molecule-fixed frame, M, has the orientation described by the eulerian angles $\Omega_0 = \alpha_0\beta_0\gamma_0$ (cf. figure 1 (B)) relative to the laboratory frame. The conditional probability $g(\Omega_0|\Omega, t)$ describes the probability that if a molecule has the orientation Ω_0 at a time $t = 0$, it has the orientation Ω at a time $t = t$. The cartesian matrix elements of $\mathbf{P}^{\mathrm{L}}(\Omega_0)$ and $\mathbf{Q}^{\mathrm{L}}(\Omega)$ are connected to the molecule fixed matrices $\mathbf{P}^{\mathrm{M}}$ and $\mathbf{Q}^{\mathrm{M}}$ through a transformation which is most conveniently performed [1–3] with the irreducible rotational matrices of Wigner [8], $D_{nm}^{(k)}(\Omega)$. In this formalism the averaging of equation (2) involves the evaluation of the angular correlation functions $\langle D_{qq'}^{(2)}(\Omega_0)D_{nn'}^{(2)*}(\Omega)\rangle$. The molecular motion of the fluorophores is described by $g(\Omega_0|\Omega, t)$. Assuming that the orientational motion around the rod-like aggregate and the local motion about the normal to the aggregate surface are statistically independent, allows the conditional probability to be written as

$$g(\Omega_0|\Omega, t) = k(\alpha_0|\alpha)\,l(\beta_0, \gamma_0|\beta, \gamma), \tag{3a}$$

where

$$k(\alpha_0|\alpha) = \frac{1}{2\pi}\sum_{q=-\infty}^{\infty}\exp(-iq\alpha_0)\exp(-t/\tau_{cq})\exp(iq\alpha) \tag{3b}$$

and within a strong collison model

$$l(\beta_0, \gamma_0|\beta, \gamma) = \{\delta(\beta - \beta_0, \gamma - \gamma_0) - f(\beta, \gamma)\}\exp(-t/\phi_c) + f(\beta, \gamma). \tag{3c}$$

τ_{cq} and ϕ_c are correlation times characterizing the rotational motions of the angles α and β, γ respectively; δ is the Dirac delta function. Equation (3 b) is the solution to the motion of a particle on a ring. In an experiment where the excitation light is polarized parallel with the director (D or Z axis), the intensities $F_{ZZ}(t)$ and $F_{ZX}(t)$ are obtained. The emission anisotropy is defined as

$$r(t) = \frac{F_{ZZ}(t) - F_{ZX}(t)}{F_{ZZ}(t) + 2F_{ZX}(t)}. \tag{4}$$

Equations (1), (3) and (4) then yield

$$r(t) = a_1 + \frac{2a_2}{a_0}\exp\left(\frac{-t}{\phi_c}\right), \tag{5}$$

where a_j are linear combinations of order parameters as given in the Appendix. In an experiment where the polarization of the excitation light is perpendicular to the director, the intensities $F_{YZ}(t)$ and $F_{YX}(t)$ are measured and the following ratio is constructed:

$$h(t) = \frac{F_{YZ}(t) - F_{YX}(t)}{F_{YZ}(t) + 2F_{YX}(t)}. \tag{6}$$

Taking the average of $F_{YZ}(t)$ and $F_{YX}(t)$ by analogy with this procedure gives

$$h(t) = \frac{a_1b_2 - a_2\exp(-t/\phi_c) + [b_0 + b_1\exp(-t/\phi_c)]\exp(-t/\tau_{c2})}{b_2 - 2[b_0 + b_1\exp(-t/\phi_c)]\exp(-t/\tau_{c2})}, \tag{7}$$

where b_j are linear combinations of order parameters as shown in the Appendix. It has been assumed that $\tau_{c2} = \tau_{c-2}$. Notice that the denominator of $r(t)$ is independent of the orientational motion of the probe molecule while this is not the case for $h(t)$.

Furthermore the symmetry of the distribution of the *excited* molecules is different in the $r(t)$ and $h(t)$ experiments. Thus, the setting of the polarizing vector parallel or perpendicular to the director generates uniaxial and biaxial distributions, respectively. The biaxial distribution created will, however, approach a uniaxial distribution at equilibrium and this situation can only be reached by motions of the fluorophores around the director, i.e. an averaging of the angle α takes place. These motions may be either the translational motion of the chromophore around the director and/or the rotational motion of the aggregate itself about its long axis. Hence, the correlation time τ_{c2}, which characterizes these motions will only appear in $h(t)$. Let us now investigate the behaviour of $r(t)$ and $h(t)$ at long times $t = t_\infty$. Suppose that the emission lifetime of the chromophore is $\tau_f \gtrsim \phi_c, \tau_{c2}$. It can then be shown that

$$r(t_\infty) = h(t_\infty) = \sum_{m=-2}^{2} \langle D_{0m}^{(2)*}(\beta, \gamma) \rangle \, d_{m0}^{(2)*}(\theta), \tag{8}$$

where $\langle D_{0m}^{(2)*}(\beta) \rangle$ are the order parameters describing the orientation of the molecular axes of the *excited* chromophore and $d_{m0}^{(2)*}(\theta)$ are the projections of the emission transition moment along these axes.

3. Experimental part

Potassium dodecanoate (laurate) was synthesized and purified using the following procedure. Decanoic acid (Merck) was vacuum-distilled three times. Decanoic acid, dissolved in ethanol of spectroscopic purity grade, was titrated with potassium hydroxide (Titrisol, p.a. quality, Merck) at *c.* 350 K. This solution was refluxed for 3 hours and the ethanol distilled off. The potassium dodecanoate was washed with ethanol and dried in vacuum. The soap was then dissolved in warm ethanol, crystallized by cooling and filtered through microfibre filters (Whatman, GF/F, 0·7 μm). The soap was again dissolved in warm ethanol and the warm solution was filtered through microfibre filters. The soap was crystallized by cooling and the warm-filtering procedure was repeated twice. The crystals were once more dissolved in warm ethanol, cooled and filtered. In order to remove dust particles a methanol solution of potassium dodecanoate was filtered under pressure through millipore filters (Millipore, FG, 0·2 μm). The solvent was evaporated and the crystals finally dried in vacuum.

The liquid crystal was composed of potassium dodecanoate, potassium chloride (dried suprapur., Merck) and ^2H_2O (99·75 at per cent ^2H, Merck) in amounts specified later. The components were mixed in test tubes that were then sealed. The samples were equilibrated by rotating them slowly at 298 K for about a week. The fluorophores were added to the fluorescence cuvettes (10 × 10 mm optical path length) by evaporating solutions of ethanol containing known concentrations of the fluorophore. The cuvettes were then filled with the liquid crystalline phase, sealed and equilibrated. Pyrene (melting point 156°C, Fluka) was recrystallized three times from diethylether. 1-dodecylpyrene and 1-pyrene dodecanoic acid were purchased from Molecular Probes Inc., Texas, U.S.A. The purity of these fluorophores were all checked with HPLC. 1-palmitoyl-2-(6-pyrenylhexanoyl)-*sn*-glycero-3-phosphorylcholine obtained from KSV-lipids (KSV-Chemical Oy, Finland) was used as received.

The fluorophore concentration in the liquid crystalline samples was 2 μM. The liquid crystals were macroscopically aligned in a magnetic field of 5·9 T for about 12 hours at 295 $\pm$ 2 K; an alignment in a magnetic field of 2·3 T (for about 20 hours) gave the same results. This strongly suggests that the samples studied have reached maximum alignment.

The polarized time-resolved fluorescence was measured with a PRA system 3000 (Photochemical Research Associates Inc., London, Ontario, Canada). The excitation source was a thyratron gated flash lamp (model 510 C) filled with deuterium and operating at about 25 kHz. The excitation wavelengths were selected by interference filters (Omega/Saven AB, Sweden) centred at 332·8 nm (HBW = 20 nm) and 335·6 nm (HBW = 8 nm). The fluorescence emission was passed through an interference filter (Saven AB, Sweden) centred at 398·8 nm (HBW = 11·4 nm). The polarized fluorescence decay curves were measured by repeated collection of data during short times, typically 200 s, for each setting of the polarizers. The excitation polarizer was fixed and the emission polarizer was periodically rotated. Data were analysed with a MINC-11 (Digital Equipment) computer using deconvolution software (DECAY V3·0a, ATROPY V1·0) developed by PRA.

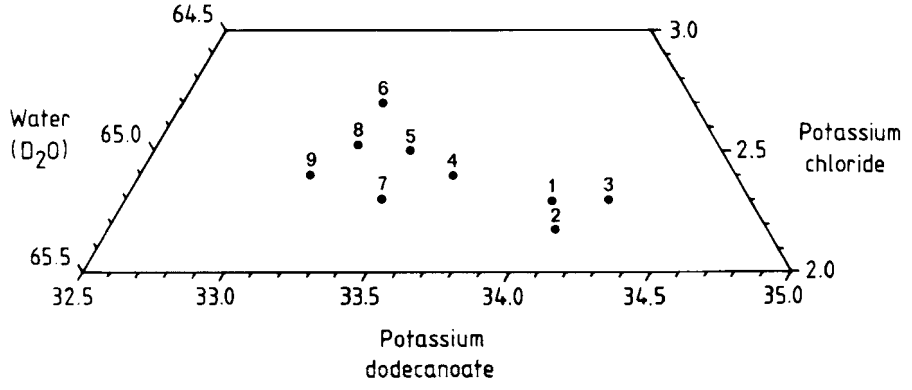

Figure 2. Partial phase diagram of potassium dodecanoate-KCl-D_2O showing the region of the magnetically orientable phase. Samples denoted 1–3 keep a constant orientation for several days.

The steady state fluorescence was recorded with a SPEX Fluorolog 112 spectrometer (SPEX Industries, Inc., Metuchen, U.S.A.). Absorption spectra were recorded on a Cary 219 (Varian, U.S.A.) spectrometer.

The samples studied are indicated in the part of a phase diagram shown in figure 2. Samples with the compositions 1–9 align macroscopically in a magnetic field. Samples in the region 1–3 keep a constant orientation for the longest periods of time, i.e. several days when thermostatted at 294 K. Only samples with compositions in this region could be utilized in this study.

4. Results and discussion

The fluorophores studied in this work are pyrene and three derivatives of pyrene namely, 1-pyrene dodecane, 1-pyrene dodecanoic acid and 2-(6-pyrenylhexanoyl)-3-palmitoyl-*sn*-glycero-1-phosphorylcholine; figure 3 shows the structure formulae of these molecules. The decay of fluorescence of the chromophores solubilized in the

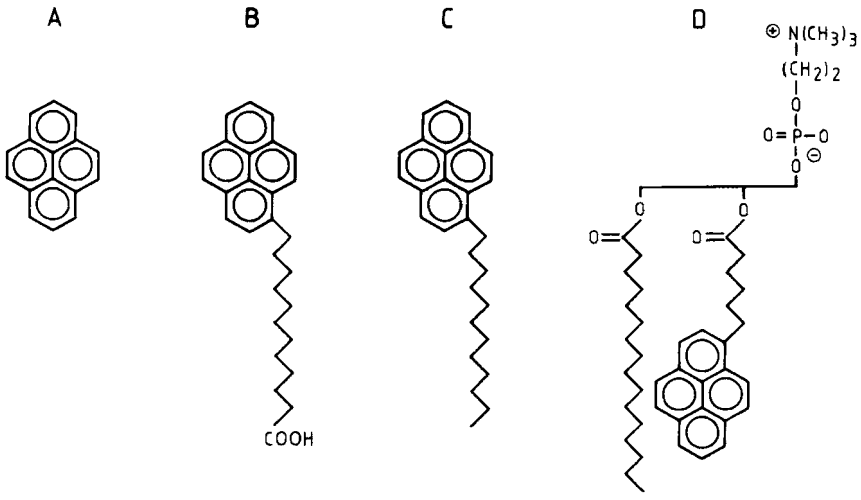

Figure 3. The fluorophores studied. (A) Pyrene. (B) 1-Pyrene dodecanoic acid. (C) 1-Dodecylpyrene. (D) 1-Palmitoyl-2-(6-pyrenylhexanoyl)-*sn*-glycero-3-phosphorylcholine.

The values of $r(t_\infty)$ and $h(t_\infty)$, the steady-state anisotropy (r_s) and the fluorescence lifetimes (τ_f) obtained for the various pyrene derivatives in the macroscopically aligned lyotropic liquid crystalline phase at 294 ± 0·5 K. The samples were not degassed.

Fluorophore	Fluorescence lifetime, τ_f/ns	Emission anisotropy $r(t_\infty)$	Steady-state emission anisotropy, r_s	$h(t_\infty)$
Pyrene	198	−0·048	−0·046	−0·048
1-Pyrene dodecyl pyrene	141	−0·039	−0·038	−0·039
1-Dodecyl pyrene	139	−0·038	−0·037	−0·037
1-Palmitoyl-2-(6-pyrenylhexanoyl)-*sn*-glycero-3-phosphoryl choline	201	−0·053	−0·055	−0·052

lyotropic nematic phase is a single exponential, ranging between 130 and 200 ns (cf. table). A typical lifetime experiment is illustrated in figure 4 (A) for the lecithin-pyrene derivative in a non-degassed sample.

Figure 4 (C) shows the emission anisotropy, $r(t)$, for the lecithin-pyrene and very similar behaviour was observed for all the different fluorophores studied. Thus, in all cases the anisotropy rapidly decreases to a stationary and negative value. Furthermore $h(t)$ is found to be identical with $r(t)$ within experimental accuracy. The observation that $r(t)$ and $h(t)$ reach the same constant value at long times is expected, since the orientational distributions of the excited chromophores must approach the *same* equilibrium distribution (see § 2). As was shown in equation (8) the plateau value of $r(t) = h(t)$ contains the order parameter characterizing the orientation of the emission transition dipole. The direction of the emission dipole moment in pyrene and some of its derivatives has recently been investigated by Langekilde *et al.* [9], who showed that the emission dipole moment is generally not polarized solely along the short axis of the molecule (y axis in figure 1 (C)) and that its direction depends on the emission wavelength. This is in agreement with our data on the emission steady-state anisotropy shown in figure 5 (B), where it can be seen that the anisotropy varies with the

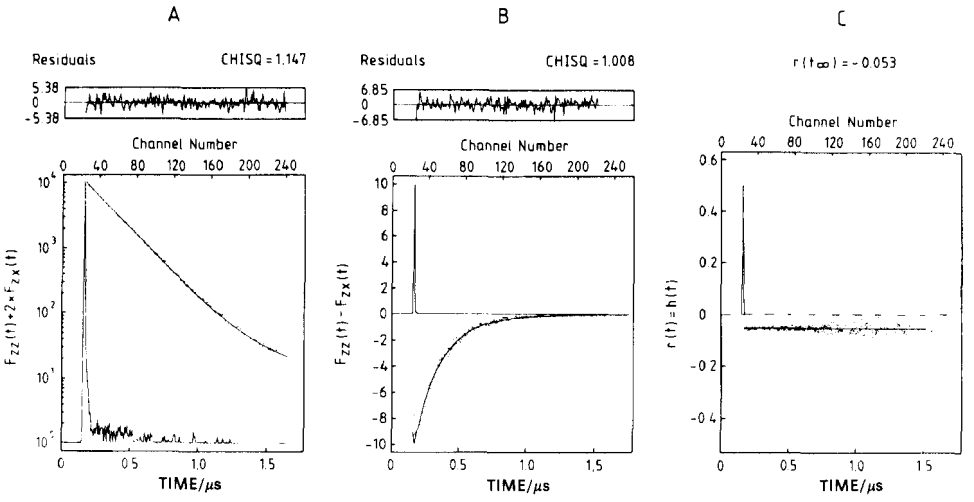

Figure 4. Time-resolved fluorescence data of 1-palmitoyl-2-(6-pyrenylhexanoyl)-*sn*-glycero-3-phosphoryl-choline solubilized in a macroscopically aligned phase. (A) Fluorescence decay, $F_{ZZ}(t) + 2F_{ZX}(t)$. (B) Difference decay, $F_{ZZ}(t) - F_{ZX}(t)$. (C) Fluorescence anisotropy $r(t)$ and the function $h(t)$ (see text).

wavelength of emission. Assuming that the emission dipole is polarized in the molecular plane (yz plane in figure 1 (C)) the negative value obtained for $r(t_\infty)$ of approximately 0·05 indicates that the plane of pyrene tends to be oriented perpendicular to the aggregate director.

The wavelength dependence on the excitation anisotropy of the lecithin-pyrene derivative is presented in figure 5 (D). This anisotropy, constructed as $(F_{ZZ} - F_{YZ})/(F_{ZZ} + 2F_{YZ})$ is obtained from the corrected steady-state intensities F_{ZZ} and F_{YZ}. Since the molecular motions of the fluorophores in the systems studied here are fast compared to the fluorescence lifetime, equation (1) can be written as

$$F \simeq k\mathbf{T}^{\mathrm{L}}\langle P_{ii}^{\mathrm{L}}\rangle\langle \mathbf{Q}^{\mathrm{L}}\rangle\mathbf{T}^{\mathrm{L},t}; \tag{9}$$

from this equation we obtain

$$\frac{F_{ZZ} - F_{YZ}}{F_{ZZ} + 2F_{YZ}} = \sum_{m=-2}^{2} \langle D_{0m}^{(2)*}(\beta\gamma)\rangle d_{m0}^{(2)*}(\theta). \tag{10}$$

It has been shown [9] that the $S_2 \leftarrow S_0(^1L_a)$ transition dipole in pyrene is directed along the long axis (z axis in figure 1 (C)). For this transition equation (10) is simple and contains only one order parameter, $\langle D_{00}^{(2)}(\beta)\rangle$, that describes the orientation of the z axis with respect to the director. $\langle D_{00}^{(2)}(\beta)\rangle = -0{\cdot}05$ is obtained, again indicating that the molecular z axis is preferentially oriented perpendicular to the director. Note, that the anisotropy remains constant in the region of the $S_2 \leftarrow S_0$ transition, which shows that the direction of the transition dipole moment is constant over the band. This is also in agreement with the results obtained for pyrene [9]. The similar and very small order parameters obtained for all the different pyrenes indicate that the orientational distribution functions are broad.

As was noted previously the time dependence on $r(t)$ ceases within a very short time compared to the time of the fluorescence decay. This implies that the local rotational motions affecting the angles β and γ are very rapid. The motions around

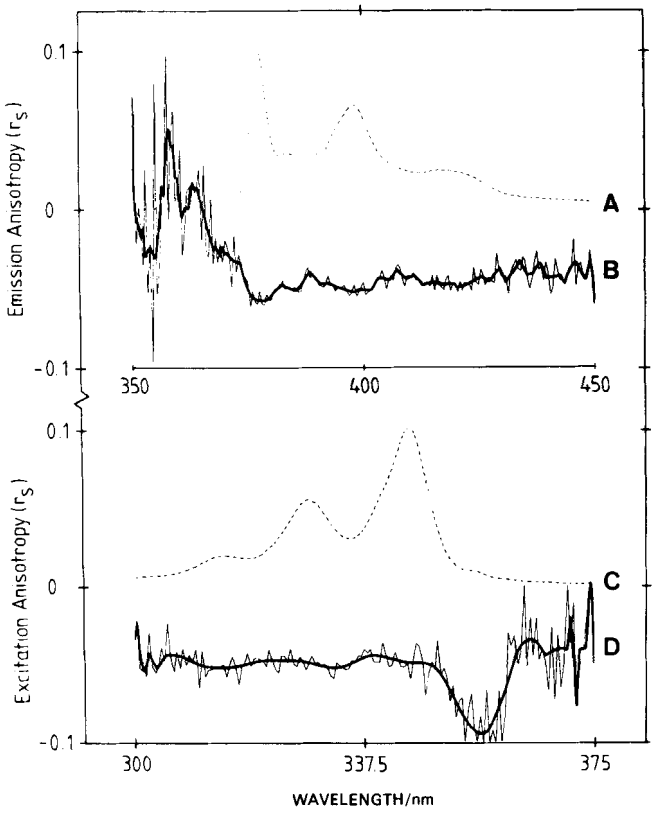

Figure 5. Steady-state fluorescence data on 1-palmitoyl-2-(6-pyrenylhexanoyl)-*sn*-glycero-3-phosphoryl-choline solubilized in a macroscopically aligned lyotropic nematic phase. (A) Fluorescence spectrum (uncorrected) recorded at the excitation wavelength 332·8 nm. (B) Emission anisotropy (r_s) obtained at the excitation wavelength 332·8 nm. Smoothed data (——). (C) Excitation spectrum (uncorrected) recorded at the emission wavelength 400 nm. (D) Excitation anisotropy obtained at the emission wavelength 400 ± 8 nm. Smoothed data (——).

the director must also be very fast, since $h(t)$, which depends on these motions, is not significantly different from $r(t)$. These motions may be either translational diffusion of the fluorophore around the director and/or rotational diffusion around the long axis of the aggregate. The correlation time for the rotation of such an aggregate can be estimated with the equations derived by Perrin [10]. A correlation time in the order of 10 μs is obtained from this equation with the length of the aggregates equal to 2000 nm, previously estimated as a lower limit from a measurement of amphiphile diffusion in this system [7], and by using the viscosity of water. Thus, the rotational motion of an aggregate around its long axis has no effect on $h(t)$ within the time scale of these experiments. The motions responsible for the averaging around the director *must therefore be translational motion* of the fluorophores. Notice that this motion is faster than the time resolution of the experiment for all the probes studied irrespectively if anchored (like pyrene dodecanoic acid and pyrene lecithin) at the aggregate surface or not (like pyrene). This is also in line with previously reported amphiphile diffusion coefficients measured by the pulsed field gradient N.M.R. method [11]. From all the data taken together it can be concluded that the translational and the

local rotational motions must have correlation times which are shorter than 20 ns. Furthermore, it can be inferred that the constant value obtained in the emission anisotropy measurements remains constant over a time longer than 1 μs. This means that over this period of time there is no other slow motion occurring, as for example a fluctuation of the normal to the surface of the rod-like aggregate or a slow wobbling motion of the director (C_∞ axis) of the nematic phase. Such a fluctuation of the director has been suggested to occur in lipid model membranes as studied by N.M.R. at various frequences [12]. Since the interpretation from N.M.R. measurements is indirect compared to the fluorescence data, where the correlation functions are obtained directly, it should be very interesting to perform an N.M.R. and a fluorescence study of this kind on the same system. Then, it should be possible to discriminate between the different motional models utilized.

We are grateful to Eva Vikström and Björn Kalman for skilful technical assistance, and to Walter Lindberg for the HPLC analysis. This work was supported by the Swedish Natural Science Research Council and the fluorescence spectrometers were financed by grants from the Knut and Alice Wallenberg Foundation and the Wenner–Gren Foundation.

Appendix

The explicit relations between the parameters a_0 to a_2, b_0 to b_2 in equations (5) and (7) and the order parameters are

$$a_0 = 1 + 2\langle D^{(2)}_{00}(\beta_0)\rangle,$$

$$a_1 = \sum_m \langle D^{(2)*}_{0m}(\beta,\gamma)\rangle d^{(2)*}_{m0}(\theta),$$

$$a_2 = \sum_m \{\langle D^{(2)}_{00}(\beta_0) D^{(2)*}_{0m}(\beta_0\gamma_0)\rangle - \langle D^{(2)}_{00}(\beta_0)\rangle\langle D^{(2)*}_{0m}(\beta\gamma)\rangle\} d^{(2)*}_{m0}(\theta),$$

$$b_0 = \frac{1}{2}\sum_m \{\langle d^{(2)*}_{20}(\beta_0)\rangle\langle d^{(2)*}_{-2m}(\beta)\exp(im\gamma)\rangle + \langle d^{(2)*}_{-20}(\beta_0)\rangle\langle d^{(2)*}_{2m}(\beta)\exp(im\gamma)\rangle\} d^{(2)*}_{m0}(\theta),$$

$$b_1 = \frac{1}{2}\sum_m \{\langle d^{(2)*}_{20}(\beta_0) d^{(2)*}_{-2m}(\beta_0)\exp(im\gamma_0) + d^{(2)*}_{-20}(\beta_0) d^{(2)*}_{2m}(\beta_0)\exp(im\gamma_0)\rangle$$
$$- \langle d^{(2)*}_{20}(\beta_0)\rangle\langle d^{(2)*}_{-2m}(\beta)\exp(im\gamma)\rangle - \langle d^{(2)*}_{-20}(\beta_0)\rangle\langle d^{(2)*}_{2m}(\beta)\exp(im\gamma)\rangle\} d^{(2)*}_{m0}(\theta),$$

$$b_2 = 1 - \langle D^{(2)}_{00}(\beta_0)\rangle.$$

The z axis of the molecular frame has been chosen parallel to the absorption transition dipole moment and the emission transition dipole is assumed to be polarized in the yz plane at an angle θ with respect to the z axis.

References

[1] Zannoni, C., Arcioni, A., and Cavatorta, P., 1983, *Chem. Phys. Lipids.*, **32**, 179.
[2] Szabo, A., 1984, *J. chem. Phys.*, **81**, 150.
[3] Johansson, L. B.-Å., and Lindblom, G., 1980, *Q. Rev. Biophys.*, **13**, 63.
[4] van der Meer, B. W., Kooyman, R. P. H., and Levine, Y. K., 1982, *Chem. Phys.*, **66**, 39.
[5] Johansson, L. B.-Å., and Lindblom, G., 1983, *J. chem. Phys.*, **78**, 1519.
[6] Cehelnik, E. D., Cundall, R. B., Lockwood, J. R., and Palmer, T. F., 1974, *J. chem. Soc. Faraday Trans. II*, **70**, 244.

[7] JOHANSSON, L. B.-Å., SÖDERMAN, O., FONTELL, K., and LINDBLOM, G., 1981, *J. phys. Chem.*, **85**, 3694.
[8] BRINK, D. M., and SATCHLER, G. R., 1968, *Angular Momentum* (Oxford University Press).
[9] LANGKILDE, F. W., THULSTRUP, E. W., and MICHL, J., 1983, *J. chem. Phys.*, **78**, 3372.
[10] CANTOR, C. R., and SCHIMMEL, P. R., 1980, *Biophysical Chemistry*, Part II (W. H. Freeman & Company).
[11] LINDBLOM, G., and WENNERSTRÖM, H., 1977, *Biophys. Chem.*, **6**, 167.
[12] BROWN, M. F., 1984, *J. chem. Phys.*, **80**, 2832.